

# Frequency shifting in free-electron lasers

G. Shvets and J. S. Wurtele

*Plasma Fusion Center and Department of Physics, Massachusetts Institute of Technology, Cambridge, Massachusetts 02139*

(Received 6 May 1993; accepted 30 September 1993)

Frequency shifting in free-electron laser (FEL) oscillators and amplifiers is investigated theoretically and numerically. The analysis includes frequency shifts from the resonant FEL interaction and the nonresonant beam dielectric. Expressions for the frequency shift in a microwave amplifier with time-dependent beam energy and current are derived and found to be in good agreement with experiments. The theory shows that temporal changes in the detuning are the dominant factor in determining the frequency shift. Electron energy fluctuations produce frequency shifts in the Compton regime, while both current and energy variations are significant in the Raman regime. The effect is particularly important for high-power microwave drivers proposed for high gradient accelerators, where the phase of the radio-frequency radiation is subject to significant constraints. FEL oscillator response to variations in beam energy is examined. It is shown that in a low-gain oscillator which experiences a sudden jump in beam energy the FEL creates spikes at the head and tail of the beam which are at the shifted frequency. The shifting is generated by time dependence in dielectric function which arises from slippage and finite lengths of the electron or optical pulse. The propagation diffusion equation is shown to describe the propagation of the spikes into the main body of the pulse.

## I. INTRODUCTION

The spectral properties of the free-electron laser (FEL) are of critical importance to many applications and have been the subject of intensive investigation. Free-electron laser sources have been proposed<sup>1</sup> with an extremely tight requirement on the bandwidth of the radiation and, for accelerator<sup>2</sup> applications, on its phase and its shot-to-shot repeatability. The FEL spectrum is governed by the nonlinear time-dependent wave-particle coupling between the beam and electromagnetic wave. Time-dependent phenomena such as sidebands<sup>3</sup> and superradiance<sup>4</sup> have been investigated theoretically and analytically. Numerical simulations have been developed to study the spectrum of the FEL over a wide range of system parameters, and well-known nonlinear phenomena such as bifurcation and chaos have also been observed. In this article, we present a theoretical model of frequency shifting in the FEL.

The frequency shifting of light by a moving dielectric front has been investigated at length theoretically<sup>5</sup> and experimentally.<sup>6,7</sup> These studies have been restricted to passive dielectric systems—those which induce phase shifts but have negligible gain. An unmagnetized plasma, where the dielectric for an electromagnetic wave is  $\epsilon = 1 - \omega_p^2/\omega^2$ , is a typical example of such a system. There is also a large body of work regarding the FEL as a dielectric medium, but until now it has been confined mainly to linear theory and optical guiding. Here we show that the dielectric picture can be fruitfully applied to time-dependent problems, leading to a deeper understanding of FEL physics. Two distinct regimes, a high-power high-gain microwave amplifier and a low-gain infrared oscillator, are studied in detail.

The amplifier theory is based on a linear FEL analysis. Under the small slippage approximation, the temporal variation of the output frequency can be calculated explic-

itly from the (changing) input parameters. Variations in current and energy produce shifts in the detuning from FEL resonance and in the beam-wave coupling. We show that it is primarily the detuning variation that determines the frequency evolution and, thus, in the Raman regime, the frequency is sensitive to both current and energy, while in the Compton regime the frequency depends mostly on the energy. The analysis predicts shifts close to those observed in recent experiments<sup>8</sup> on a microwave FEL.

The FEL power in an oscillator will grow from either beam noise or spontaneous emission. The radiation pulse length and amplitude are governed by the slippage parameter, the cavity detuning, and the net gain: Here we investigate the response to either a jump or a slow modulation of the input electron energy *after* the radiation has first grown, typically with a spectrum centered around the maximum gain frequency. After the energy jumps suddenly, the optical pulse is detuned and its gain cannot compensate for its losses. Clearly, the FEL will respond by changing the center frequency of the optical pulse. A few physical mechanisms may be responsible for this: Random noise may be present at the new operating frequency and amplified while the original signal decays, or a synchrotron sideband may be present near the new frequency and amplified.

Our numerical studies and analytic work show that frequency shifting causes the change in the spectrum, which requires neither beam noise nor an initial low-power signal near the new operating frequency. For the first time, the process by which the “proper” frequency spreads into the bulk of the pulse is identified as a diffusion process, and its rate is estimated. The diffusion model shows that in the low-gain regime the system responds to a sudden change in detuning by establishing the new peak gain frequency at the wings of the pulse where slippage is significant, and gives a good estimate for the rate at which the correct

frequency propagates inwards to the center of the pulse. This result agrees with numerical simulation. The spikes that occur at the edges of the pulse are analogous to the superradiant<sup>4</sup> spikes in high-gain amplifiers.

Recently, Darrow, *et al.*<sup>9</sup> have examined the backscattered light from the strong electromagnetic wave launched into plasma using a time-dependent frequency shifting approach.

The theoretical model is presented in Sec. II, amplifier analysis is given in Sec. III, oscillators are examined in Sec. IV, and our conclusions are presented in Sec. V.

## II. THEORETICAL MODEL

This section contains the basic theoretical model used to describe the pulse evolution in an FEL. The system is assumed to be one-dimensional, with a helical wiggler and circularly polarized electromagnetic (EM) wave. The fundamental equations used herein to describe the FEL interaction are the well-known<sup>3</sup> eikonal equations. The wave equation for the vector potential is

$$\left( \frac{1}{c^2} \frac{\partial^2}{\partial t^2} - \frac{\partial^2}{\partial z^2} + k_1^2 \right) \mathbf{A} = \frac{4\pi}{c} (\mathbf{J}_{\text{nr}} + \mathbf{J}_{\text{fel}}), \quad (1)$$

where the source term has two distinct contributions:  $\mathbf{J}_{\text{nr}}$ , from the (nonresonant) cold beam response to the electromagnetic wave, which is present in the absence of the wiggler, and a second term from the resonant FEL interaction. The resonant current  $\mathbf{J}_{\text{fel}}$  is produced by the ponderomotive force of the electromagnetic wave beating with the magnetic field of the wiggler.<sup>10</sup> The beam is bunched in this ponderomotive wave, and the wiggling bunches produce the current which drives the wave synchronously. This results in an exponentially growing instability when the response is linear. Since the parameters of the electron beam can be time-dependent, frequency-changing phenomena may result.

It is worthwhile to briefly summarize frequency shifting in passive media, such as occurs when radiation propagates through a moving inhomogeneous medium<sup>11,12</sup> with no FEL interaction. The wave equation, when used together with canonical momentum conservation, becomes

$$\left( \frac{1}{c^2} \frac{\partial^2}{\partial t^2} - \frac{\partial^2}{\partial z^2} + k_1^2 \right) \mathbf{a} = -\frac{\omega_p^2(z,t)}{c^2} \mathbf{a}, \quad (2)$$

where we have introduced the normalized vector potential of the radiation field  $\mathbf{a} = e\mathbf{A}/mc^2$ ,  $e$  is the electron charge,  $m$  is the electron mass,  $c$  is the speed of light in vacuum,  $\omega_p^2(z,t) = 4\pi e^2 n(z,t)/m$  is the nonrelativistic beam plasma frequency, and  $n(z,t)$  is the beam density.

It is convenient to transform to variables  $(s,z)$  defined by

$$s = t - \frac{z}{v_g}, \quad z = z, \quad (3)$$

where  $s$  is the distance from the head of the wave packet, which propagates with group velocity  $v_g$ . Using the eikonal approximation, which in our notation requires that variations in  $z$  be much slower than in  $s$ , results in

$$\frac{\partial a(s,z)}{\partial z} = -\frac{i\omega_p^2(s,z)v_g}{2\omega c^2} a(s,z). \quad (4)$$

While it is straightforward to integrate Eq. (4) by quadratures, further insight can be obtained by assuming that the density gradient is moving with constant velocity,  $v_b$ . In this case, for a prescribed density profile  $\omega_p^2(t-z/v_b)$

$$a(s,z) = a(s,0) \exp[-i\Phi(s,z)] \quad (5)$$

and the frequency change,  $\delta\omega = \partial\Phi/\partial s$ , is now given by

$$\delta\omega(s,z) = \frac{\beta_b\beta_g}{2\omega(1-\beta_b/\beta_g)} \left[ \omega_p^2(s) - \omega_p^2\left(s - \frac{z(1-\beta_b/\beta_g)}{v_b}\right) \right]. \quad (6)$$

It is instructive to analyze this equation in two limits. First, expanding the term  $\omega_p^2[s - z(1-\beta_b/\beta_g)/v_b]$  in Eq. (6) results in an expression for the frequency change of a pulse that has propagated a distance  $z$  with the moving plasma

$$\delta\omega(s,z) = \beta_g \frac{1}{\omega} z \frac{\partial\omega_p^2}{\partial(cs)}. \quad (7)$$

This expression is well behaved for  $v_g = v_b$ , and our subsequent analysis of the FEL amplifier in Sec. III will be carried out under this "zero slippage" assumption. Second, the opposite limit, that of a step profile electron beam, where finite slippage generates the frequency shift, can also be recovered from Eq. (6). Radiation which starts inside the electron beam and eventually slips out of the beam because  $v_g > v_b$ , is frequency upshifted by

$$\delta\omega = \frac{\beta_b\beta_g}{1-\beta_b/\beta_g} \frac{\omega_p^2}{2\omega}. \quad (8)$$

In Sec. IV this equation will be used to estimate the effect of nonresonant beam dielectric terms on the FEL oscillator spectrum.

Unfortunately, when the FEL interaction is included, the differential equation for the vector potential is no longer first-order, and a simple integration, similar to the one above, is no longer possible. The above two cases give us, nevertheless, a good physical understanding of how the frequency changes are brought about when different longitudinal slices of radiation evolve differently. For example, in the zero slippage limit, longitudinal slices of radiation can interact with different electron densities, and thus acquire differing phase changes on a single pass. In the large-slippage case, slices of radiation that are different distances away from the head of the electron bunch, in the absence of the FEL interaction, receive phase shifts which increase towards the head of the pulse (since plasma has a negative refraction index).

## III. FEL AMPLIFIER

In this section we restrict our analysis to amplifiers. The theory will be applied to a microwave FEL experiment operating in a single waveguide mode, with time-dependent system parameters. A key simplification will be the zero slippage  $S = L_{\text{slip}}/L_{\text{beam}} \approx 0$  approximation, where  $L_{\text{slip}} = [(\beta_g/\beta_b) - 1]L_w$  and  $L_{\text{beam}}$  is the length of the elec-

tron beam. This is reasonable for many microwave FELs, which have long pulse lengths, moderately relativistic energies, and a reduction of the group velocity in the waveguide. For instance, in recent spectral studies of a microwave FEL,<sup>8</sup> the slippage parameter is less than 5%. The FEL equations, which have temporal and spatial derivatives in the field equation, then become ordinary differential equations.<sup>4</sup>

The amplifier analysis is based on previous work,<sup>13</sup> and includes the effects of waveguide modes, space charge, and axial guide magnetic fields in a helical wiggler geometry. Following previous work,<sup>13</sup> the nonlinear FEL equations are, in the eikonal approximation,

$$\frac{\partial \gamma_j(z)}{\partial z} = iC \frac{\beta_{\perp 1}}{2\beta_{\parallel 1}} a(z, s_j) \exp(i\theta_j) - i \frac{\omega_p^2(s) p_1^2}{c^2 (k_z + k_w)} \exp(i\theta_j) \times \langle \exp(-i\theta_j) \rangle + \text{c.c.}, \quad (9)$$

$$\frac{\partial \theta_j(z)}{\partial z} = k_z + k_w - \omega/v_{\parallel j}, \quad (10)$$

$$\frac{\partial a}{\partial z} + iF \frac{\omega_p^2(s)}{2\gamma\omega v_b} \frac{\omega - k_z v_b}{\omega - k_z v_b - \Omega_0/\gamma} a \underbrace{= 2\pi i C \frac{I(s)}{I_A} \left\langle \frac{\beta_{\perp 1}}{\beta_{\parallel 1}} \exp(-i\theta_j) \right\rangle}_{\text{fel}}, \quad (11)$$

where  $v_{\parallel} = \beta_{\parallel} c$  is the longitudinal electron velocity,  $\theta_j = (k_z + k_w)z - \omega t_j$  is the slow varying ponderomotive phase,  $a(z, s)$  is proportional to the eikonal of the vector potential,  $v_b$  is the unperturbed beam velocity,  $\gamma$  is the beam relativistic factor,  $\Omega_0 = eB_0/mc$  is the cyclotron frequency due to the axial field  $B_0$ ,  $F$  is a dimensionless filling factor,  $C$ , a geometric factor<sup>13</sup> which depends on the waveguide and mode, is

$$C = \left( \frac{k_0 p_{11}^2}{2\pi k_z z_g^2 (p_{11}^2 - 1) J_1^2(p_{11})} \right)^{1/2}, \quad (12)$$

and  $p_{11}'$  is the first zero of  $J_1'(z)$ . The factor  $C$  roughly equals the inverse of the waveguide radius. A nonresonant beam-loading term, which is not present in earlier work,<sup>13</sup> has been included in Eq. (11). Equations (9)–(11) can be easily linearized in the approximation where force bunching and wave perturbation of the equilibrium orbits is negligible. The dispersion relation thereby obtained (including the beam-loading term) is

$$\left( \Gamma + F \frac{\omega_p^2(s)}{2\gamma\omega v_b} \frac{\omega - k_z v_b}{\omega - k_z v_b - \Omega_0/\gamma} \right) \left( (\Gamma + \Delta K)^2 - \frac{1}{\beta_{\parallel 0}} \frac{\partial \beta_{\parallel 0}}{\partial \gamma} \frac{p_1^2 \omega_p^2}{c^2} \right) = - \frac{\pi C^2 \beta_{\perp 1}^2}{\beta_{\parallel 0}^4 c I_A} I \omega \frac{\partial \beta_{\parallel 0}}{\partial \gamma}. \quad (13)$$

Here

$$\Delta K = k_z + k_w - \omega/v_{\parallel 0} \quad (14)$$

is the unperturbed energy detuning.

When the electron beam density and energy change slowly and remain close to their peak-gain values

$$\begin{aligned} \omega_p^2(s) &= \omega_{p0}^2 + \Delta\omega_p^2(s), \\ \gamma &= \gamma_0 + \delta\gamma. \end{aligned} \quad (15)$$

Solving for the real part of the gain, which determines the phase change of the radiation and thus the frequency change, we obtain

$$\text{Re}(\Gamma) = \frac{\Gamma_{\text{sp}} - \Gamma_{\text{nr}} - \delta(\Delta K)}{2}. \quad (16)$$

Here,  $\Gamma_{\text{nr}}$  results from the nonresonant time-dependent beam-loading [with the  $\mathbf{J}_{\text{nr}}$  in Eq. (1) as a source],  $\Gamma_{\text{sp}}$  describes the time-dependent coupling to the slow space-charge wave, and  $\delta(\Delta K)$  is the time-dependent change in the detuning. Explicitly

$$\Gamma_{\text{nr}} = F \frac{\Delta\omega_p^2(s)}{2\gamma\omega v_b} \frac{\omega - k_z v_b}{\omega - k_z v_b - \Omega_0/\gamma}, \quad (17)$$

$$\Gamma_{\text{sp}} = \left( \frac{1}{\beta_{\parallel 0}} \frac{\partial \beta_{\parallel 0}}{\partial \gamma} \right)^{1/2} p_1 \Delta\omega_p(s)/c, \quad (18)$$

and

$$\delta(\Delta K) = \frac{\omega}{c\beta_{\parallel 0}^2} \frac{\partial \beta_{\parallel 0}}{\partial \gamma} \delta\gamma. \quad (19)$$

The particle dynamics along the unperturbed trajectory are characterized<sup>13</sup> by

$$\frac{\partial \beta_{\parallel 0}}{\partial \gamma} = \frac{1}{\gamma\beta_{\parallel 0}} \left( \frac{1}{\gamma_{\parallel}^2} + \frac{x}{1-x} \right), \quad (20)$$

where

$$x = \frac{c^2 k_w^2 \Omega_0}{(c\beta_{\parallel 0} k_w \gamma - \Omega_0)^3}. \quad (21)$$

The frequency change after an interaction length  $z$  is

$$\delta\omega_{\text{ram}} = -\frac{1}{2} z \frac{\partial(-\Gamma_{\text{nr}} + \Gamma_{\text{sp}} - \delta\Delta K)}{\partial s}. \quad (22)$$

This equation shows that the frequency shift occurs because of two distinct mechanisms: the usual cold beam nonresonant shift (from the beam density) and the shift from resonant coupling to the slow space-charge wave, which is due to the FEL interaction. The beam dielectric shift is physically equivalent to that of a cold plasma, and has been extensively described in the literature.<sup>14</sup> The FEL-induced shift has not been analyzed previously.

It is interesting to compare the physical origin of the frequency shift from the nonresonant beam loading with that of the purely Raman FEL shift. In Fig. 1, an electron beam is shown moving to the right with a density increasing towards its tail. At the head of the pulse, the peaks of the EM wave have a phase velocity slower than those further back. This results in peaks at the tail catching up with peaks at the head, and, therefore, in a frequency upshift. In contrast, the Raman FEL interaction produces a downshift with the *same* moving density gradient. The radiation cou-

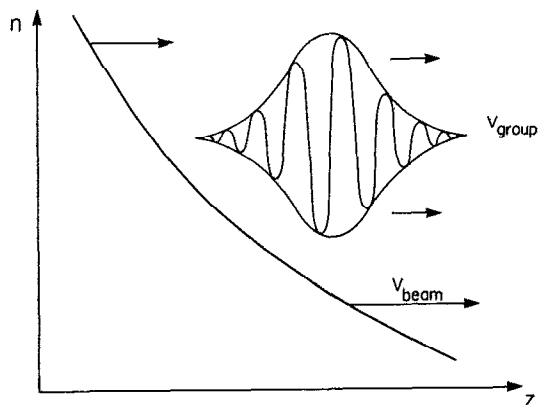


FIG. 1. A radiation pulse riding on a beam with a temporally increasing density gradient is continuously frequency upshifted.

ples to the slow space-charge wave, whose phase velocity becomes slower as the beam density increases. Adjacent radiation peaks now move farther apart with increasing interaction distance, and the frequency downshifts. This can also be seen from signs of the different terms that generate frequency shifts in Eq. (22).

The derivation of an expression for frequency shifting in the Compton FEL can be carried out by following the steps leading to Eq. (22). The result is

$$\delta\omega_{\text{comp}} = \frac{z}{3} \frac{\partial[\Gamma_{\text{nr}} + 2\delta(\Delta K)]}{\partial s} \quad (23)$$

From Eq. (23), it is clear that, for a Compton FEL, the only resonant contribution to phase shift comes from the energy variation. Yet from Eq. (22) we see that resonant contributions to the phase shift come from both current and energy variations. We also notice that if the slope of the current and the energy variation both have the same sign, the resulting frequency shifts will have opposite signs. These observations will become important in the next section, where we analyze an FEL experiment,<sup>8</sup> and infer that the difference in the magnitude of frequency shifts in different operating regimes is related to a change from the strongly Raman regime to a nearly Compton regime FEL. In general, the nonresonant shift is smaller than the resonant shifts.

Our theory can be complemented by the results of a *single-frequency* numerical simulation (provided the zero slippage approximation is valid). A numerical code can be used to obtain the phase of the radiation, at a given spatial location in the FEL amplifier, as a function of the initial electron energy and current. Then, assuming a known dependence of the input parameters on time, we can deduce the resulting frequency changes. This procedure yields shifts that include such important effects as nonlinear saturation, finite beam emittance, energy spread, particle loss and three-dimensional particle motion, and waveguide modes. It is employed in the analysis of experimental results in the next section.

*Frequency shifting in an amplifier experiment.* Frequency shifts of the order of  $\delta f = 80$  MHz have been re-

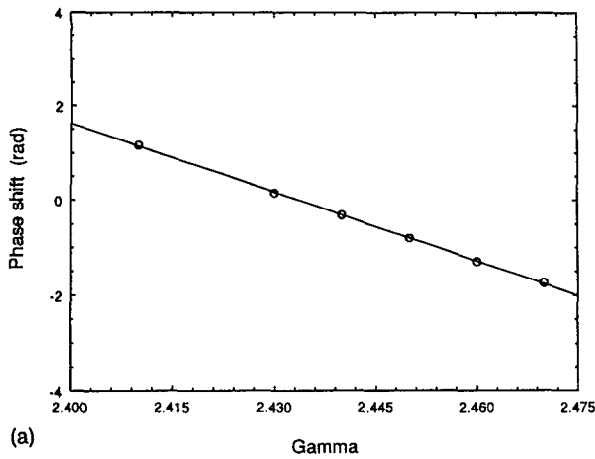
ported in recent experiments.<sup>8</sup> In these measurements, a magnetron provided a  $\approx 30$   $\mu\text{s}$  monochromatic signal at a frequency  $f_0 = 33.39$  GHz input to the FEL amplifier. In the group I parameter regime, the amplified power was measured to be at the frequency  $f_0 + \delta f = 33.47$  GHz. The upshifting was much smaller in the reversed field regime.<sup>15</sup> Recent measurements<sup>16</sup> show that the frequency upshift in this regime does not exceed  $\approx 10$  MHz. It was also shown experimentally that the spectrum of the output radiation shifted towards higher frequencies monotonically with increasing interaction length, and measurements were carried out in the linear regime before saturation and particle trapping. This precludes sidebands as an explanation of the shift. The frequency shift was also seen to track the input frequency, which rules out a growth of beam noise at a particular frequency as an explanation.

The slippage in these experiments is about 5% and, therefore, the amplifier analysis described above is applicable. The experimental data can be compared to theory by using the results of a three-dimensional simulation<sup>17</sup> code to find the dependence of the phase on the beam current and energy. The concomitant frequency shifts can then be obtained from the phase calculations through simple differentiation if the time dependence of the current and energy are known. Experimental evidence<sup>16</sup> exists to show that the frequency upshift of the radiation occurs primarily when both the anode-cathode voltage (and thus the electron energy) and the electron current are still *increasing*. In order to estimate the magnitude of the shifts, we assume that the voltage and current sweep across a gain bandwidth over a time  $\approx 20$  ns, which is consistent with the measured pulse length. The sweep involves choosing the upper and lower boundaries for current and electron energy such that the output power is reduced by a factor of 2.7. The results are shown in Fig. 2. We note from Figs. 2(a) and 2(b) that changes in the phase,  $\phi$ , from current and energy variations in the reversed field regime almost cancel each other out, resulting in a very small ( $\Delta\nu = \Delta\phi/20$  ns  $< 10$  MHz) frequency shift. In Fig. 2(c), for group I parameters, the phase is plotted as a function of input beam energy. From the phase shift, we estimate an 80 MHz frequency shift, which agrees well with the predictions of the linear theory from Eq. (23). Both the reversed field and group I estimates are close to the experimentally observed<sup>8</sup> upshifts.

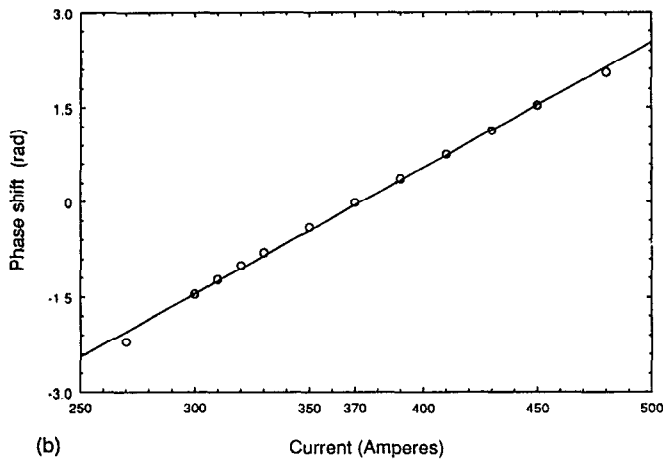
The difference between the two measurements can be easily understood. When the FEL is operated in the group I regime,<sup>8</sup> it is primarily in the Compton regime, where the only resonant contribution to the frequency shift comes from the energy variation. On the other hand, when operated in the reversed field regime, the FEL is strongly Raman, so that resonant contributions come from both the current and the energy variations, which can cancel each other out, since they have opposite signs.

#### IV. OSCILLATORS

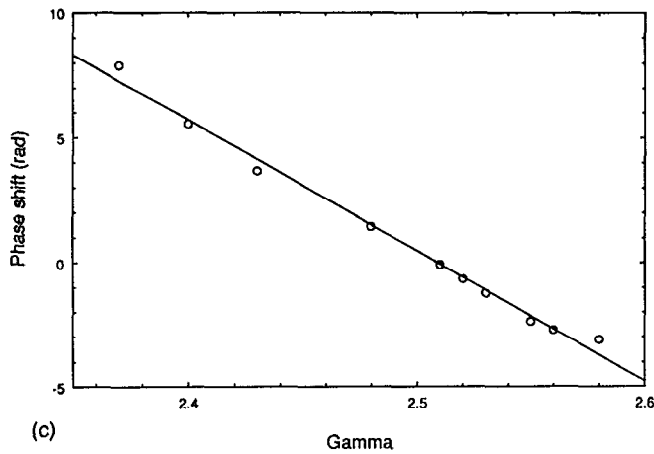
Free-electron oscillators at infrared and shorter wavelengths generally operate with finite slippage and very small space-charge forces and, often, a single-pass gain less than unity. Time dependence of the beam parameters can



(a)



(b)



(c)

FIG. 2. Phase of the radiation after an interaction length of 150 cm as a function of (a) electron energy in the reversed field regime, (b) current in the reversed field regime, and (c) electron energy in the group 1 regime.

produce frequency changes from both  $\mathbf{J}_{nr}$  and  $\mathbf{J}_{fel}$ . Furthermore, even if the beam parameters are completely time-independent, slippage will generate frequency shifts from only the FEL interaction whenever the optical pulse is nonuniform. In the analysis below these effects will be isolated and analyzed independently.

Frequency shifting from  $\mathbf{J}_{nr}$  is present in the absence of the wiggler. Light bouncing between two mirrors will interact with a fresh electron pulse once each round-trip, and

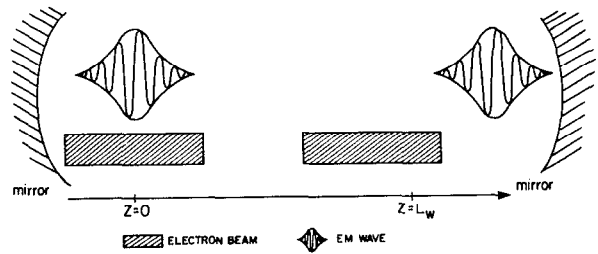


FIG. 3. Schematic for the continuous frequency shift of a flattop radiation pulse. The spacing between electron bunches is assumed to be equal to the round-trip of the radiation pulse.

can thus undergo successive frequency shifts as it slips over an electron pulse during each pass. This is shown in Fig. 3, which presents an interesting example of a cumulative frequency upshift. The spacing between the mirrors (cavity detuning) is such that an optical pulse overlaps a flattop electron pulse at the front mirror and completely slips over it by the end of the cavity. The light pulse will be frequency upshifted by an amount  $\delta\omega$  given by Eq. (8). If the cavity is tuned in such a way that the temporal spacing between the successive electron bunches is equal to the round-trip of light through the cavity, then on the next pass the pulse will overlap the next bunch again, and the upshifting will repeat itself. Thus, such upshifting is cumulative and, over many passes, can significantly alter the frequency of the radiation. If the slippage parameter is, say, one-half, then only the front portion of the wave is upshifted, whereas the tail will not change its frequency. This mechanism may conceivably be used for fine tuning of the optical frequency and for chirping pulses. The practical use of the nonresonant beam to frequency shift an optical pulse will require, of course, that the shifts be obtained before the pulse decays from cavity losses.

It appears, at first glance, that frequency shifting might be very deleterious to the operation of an FEL oscillator. It might detune the light far off resonance, thereby terminating the interaction; this is a surprising result in view of the successful operation of many FEL oscillators. In fact, the frequency shifts are limited by a number of various effects, such as laser lethargy,<sup>18</sup> where the FEL interaction modifies the group velocity of the radiation, and the smallness of the nonresonant beam phase shift compared with the FEL phase shift. Lethargy results in the pulse slipping back on the electron bunch, and it is usually compensated for by shortening the cavity so that it is less than half of the interbunch separation (cavity detuning). Then radiation at a given position  $s$  will eventually stop overlapping electron bunches by moving ahead of or behind them, depending on the relative sizes of cavity detuning and laser lethargy. As a rough estimate, a radiation slice which overlaps the bunch must have originated within

$$\mathcal{N}_{\text{eff}} \approx \frac{S}{|(\Delta\beta_g 2\gamma_{\parallel}^2 - 2\Delta l/L_{\text{slip}})|} \quad (24)$$

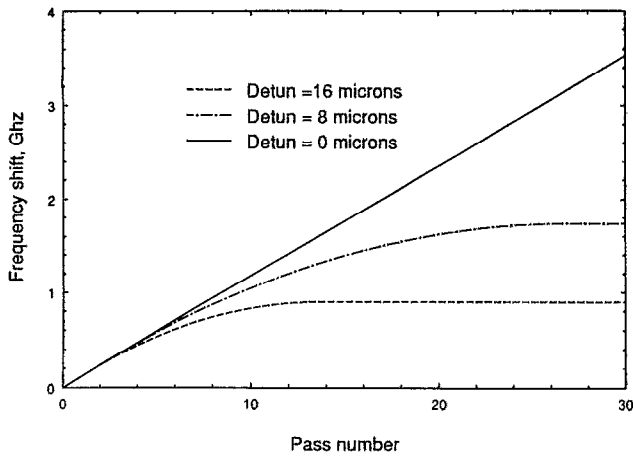


FIG. 4. Cumulative frequency upshift of a flattop radiation pulse as a function of cavity detuning. The FEL interaction has been turned off.

previous passes. The slippage parameter  $S$  is defined by  $S = L_{\text{slip}}/L_{\text{beam}}$ ,  $\Delta\beta_g$  is the group velocity reduction due to lethargy, and  $\Delta l$  is the cavity detuning.

The maximum frequency shift that can develop is then, roughly

$$\Delta\omega \approx \mathcal{N}_{\text{eff}} \delta\omega, \quad (25)$$

where  $\delta\omega$  is given by Eq. (8), and  $S \gg 1$  is assumed. The shift of the mean frequency of a radiation pulse interacting with successive flattop electron bunches *only* through the beam loading (no FEL) is plotted as a function of the pass number in Fig. 4 for various cavity detunings. The results in Fig. 4 are obtained from a one-dimensional time-dependent FEL simulation code<sup>19</sup> which was modified to include the nonresonant beam interaction. This plot clearly shows “saturation” of the frequency shift when  $n_{\text{pass}} > \mathcal{N}_{\text{eff}}$ . There will be a similar frequency shift, with  $\delta\omega$  given by Eq. (7), even for  $S \ll 1$ , whenever the beam has a density gradient.

We now examine frequency changes which do not require any temporal dependence of the beam parameters. These slippage-driven frequency-changing phenomena develop from the nonlocal character of the FEL interaction. The physics is easy to understand: Each radiation slice leaves behind it a wake which influences trailing radiation up to a distance  $\Delta L = N_u \lambda_s$  behind it.

It is convenient to normalize the coordinates ( $z, s$ ) [from Eq. (3)], to the wiggler length and the slippage length, respectively. Thus

$$\begin{aligned} \bar{z} &= z / (N_u \lambda_w), \\ \bar{s} &= 2\gamma_{\parallel}^2 s / (N_u \lambda_w). \end{aligned} \quad (26)$$

Coarse graining on the scale of a round-trip gives a very general equation for the time-dependent FEL [see the Appendix, Eq. (A10)]

$$\frac{\partial \hat{a}}{\partial n} = -\delta \hat{a} + \hat{a} \hat{G} - i \frac{\partial \hat{a}}{\partial \bar{s}} \frac{d \hat{G}}{d \bar{y}_0} - \frac{1}{2} \frac{\partial^2 \hat{a}}{\partial \bar{s}^2} \frac{d^2 \hat{G}}{d \bar{y}_0^2}, \quad (27)$$

where  $y_0 = (k_w - k_z / 2\gamma_{\parallel}^2) L_w$  is the detuning from resonance, defined as the change in the ponderomotive phase seen by an electron moving through the wiggler of length  $L_w$ ,  $\delta$  is the intracavity loss per pass, and  $n$  is the pass number. For maximum gain,  $y_0 \approx 2.6$ . The function  $\hat{G}$  is a complex gain function

$$\begin{aligned} \hat{G}(y_0) &= i j_c \int_0^1 d\bar{z} \exp(-iy_0 \bar{z}) \\ &\quad \times \int_0^{\bar{z}} d\bar{z}' \int_0^{\bar{z}'} d\bar{z}'' \exp(iy_0 \bar{z}''), \end{aligned} \quad (28)$$

where  $j_c$  is a coupling parameter

$$j_c = 8\pi N^3 \frac{I}{I_A} \frac{\lambda_w^2 a_w^2}{r_b^2 \gamma^3}$$

and  $r_b$ ,  $\lambda_w$ ,  $I$ , and  $I_A$  are the beam radius, wiggler wavelength, current, and Alfvén current, respectively. An equation similar to Eq. (27) was analyzed in the context of the supermode theory,<sup>20</sup> but only for a specific electron beam current profile, and not to study frequency shifting phenomena.

We are now in a position to examine the importance of the nonresonant phase shift from beam-loading compared to the FEL-induced phase shift. It is easy to show from Eq. (28) that the total phase shift at resonance (where it is the largest) is given approximately by  $\Delta\phi_{\text{nr}} = G_{\text{max}}/1.65$ , where  $G_{\text{max}}$  is the peak gain at  $y_0 \approx 2.6$ . The nonresonant phase shift can be estimated as

$$\Delta\phi_{\text{nr}} = \frac{NI(1+a_w^2)}{\gamma^3 I_A} \frac{\lambda_w^2}{r_b}. \quad (29)$$

For the typical parameters that were used in our numerical investigations,  $I = 60$  A,  $\lambda_w = 5.0$  cm,  $N = 40$ ,  $r_b = 1$  mm,  $\gamma = 59$ ,  $\lambda_s = 1$   $\mu\text{m}$ , and the ratio  $\Delta\phi_{\text{nr}}/\Delta\phi_{\text{fel}} \approx 3 \times 10^{-3}$ . Thus, the effect of the nonresonant correction is negligible. We note that this may not always be the case, since at fixed low gain the ratio

$$\Delta\phi_{\text{nr}}/\Delta\phi_{\text{fel}} = \frac{6(1+a_w^2)}{\pi N^2 a_w^2} \quad (30)$$

may increase with the use of microwigglers. The net result of including the nonresonant phase shift is a slight change in the operating frequency of the FEL. For the above parameters this correction is within a  $10^{-4}$  bandwidth.

*Examples of frequency shifting in oscillators.* Equation (27) describes the response of the FEL to changes in system parameters. Consider, for example, an idealized system in which a beam consisting of flattop electron bunches is injected at an energy detuned from the peak-gain energy of the radiation pulse already present in the laser. It is clear that the evolution of radiation slices within a slippage distance of the head or tail of the pulse can differ from that of the bulk. Both the numerical simulation and the diffusion equation (31) (below) show that the front and back of the signal will experience frequency shifts which bring them closer to the maximum gain condition. As a consequence, two spikes, at the front and at the end will appear and grow

at a faster rate than the bulk of the pulse. Eventually, the spikes spread over the entire pulse, thus establishing the “right” (peak gain) frequency everywhere. This scenario is based solely on the wake-like nature of the FEL interaction. If the electron bunch is not substantially longer than the radiation pulse, additional frequency shifts from temporal variations of beam parameters must be included.

A simple analytical expression which describes the evolution of the pulse can be obtained in the limit of a long electron bunch. A few assumptions will further simplify the analysis. The frequency is assumed to be near its peak-gain value (where the real part of the complex gain  $\hat{G}$  has a maximum), so that the complex gain [from Eq. (28)] and its derivatives can be estimated at  $y_0 \approx 2.6$ . Also, even though the inflection point of the imaginary part of  $\hat{G}$  is at  $y_0 \approx \pi$ , the second derivative of the gain function is approximately a real number. The first two terms in the RHS of Eq. (27) are eliminated when intracavity loss exactly matches the maximum growth rate. Neither of these assumptions affect the profile itself, but would multiply the result by a constant after every pass.

The solution to Eq. (27) is particularly straightforward in a frame propagating in the positive  $s$  direction with a speed  $|d\hat{G}/dy_0|$ . Equation (27) becomes

$$\frac{\partial \hat{a}}{\partial n} = \frac{1}{2} q \frac{\partial^2 \hat{a}}{\partial s^2}, \quad (31)$$

where  $q = d^2\hat{G}/dy_0^2$ , evaluated at  $y_0 \approx 2.6$ . The solution to Eq. (31) is given by the convolution of the Green's function for the diffusion equation and initial condition at  $n=0$

$$\hat{a}(n,s) = \int_{-\infty}^{+\infty} ds' \hat{a}_0(s') \frac{\exp[-(s-s')^2/2qn]}{(2\pi qn)^{1/2}}. \quad (32)$$

The pulse initially extends from  $s=0$  to  $s=T$  and has the form of

$$\hat{a}(s) = \exp(i\Delta s),$$

where  $\Delta \approx 2.6 - y_0$  is a detuning from the maximum gain. Then the amplitude and the phase of the pulse after  $n$  passes is given by

$$|\hat{a}(s)| = \left[ \left( \int_{s-T}^s ds' \cos(\Delta s') \frac{\exp[-s'^2/2qn]}{(2\pi qn)^{1/2}} \right)^2 + \left( \int_{s-T}^s ds' \sin(\Delta s') \frac{\exp[-s'^2/2qn]}{(2\pi qn)^{1/2}} \right)^2 \right]^{1/2}, \quad (33)$$

$$\phi(s) = \Delta s - \tan^{-1}$$

$$\times \frac{\int_{s-T}^s ds' \sin(\Delta s') \exp(-s'^2/2qn) / (2\pi qn)^{1/2}}{\int_{s-T}^s ds' \cos(\Delta s') \exp(-s'^2/2qn) / (2\pi qn)^{1/2}}. \quad (34)$$

These integrals are error functions of a complex argument, and are numerically evaluated as shown in Fig. 5. We see that the formation of the spikes at the edges of the injected pulse is concomitant with the frequency changing, and that

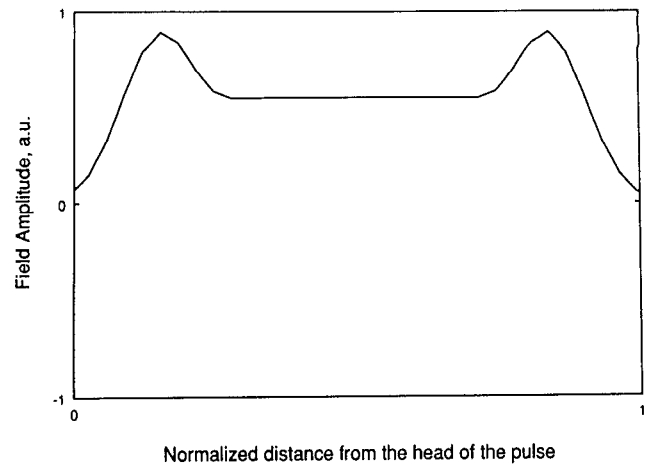


FIG. 5. Spike formation, 20 passes after a jump in detuning, as predicted by the diffusion equation.

the interior of the pulse, which is not subject to a frequency shift, decays much faster than the edges. Simulation results for a similar set of parameters, where an EM pulse has been positioned deep inside an electron bunch, so that end effects are negligible, are shown in Fig. 6. Comparing Fig. 5 and Fig. 6, we see that the diffusion-like equation captures the main features of the full-scale numerical simulation. The analytical results cannot be applied for long evolution times because of the neglected higher-order  $s$  derivatives, which make the evolution equation causal (see the Appendix). We note that a diffusion equation for a *complex* quantity can produce spikes of its absolute value, while this is not the case for the diffusion of a real quantity.

A more complicated picture is obtained when finite bunch lengths are included. In such a case, depending on the relative size of the laser lethargy and cavity detuning, one of the spikes (either a front spike, or superradiant tail spike) dominates. This is clearly shown in Figs. 7 and 8, for which detunings are chosen to be 5 and 25  $\mu\text{m}$ . A detailed analysis of the relative contributions of finite EM

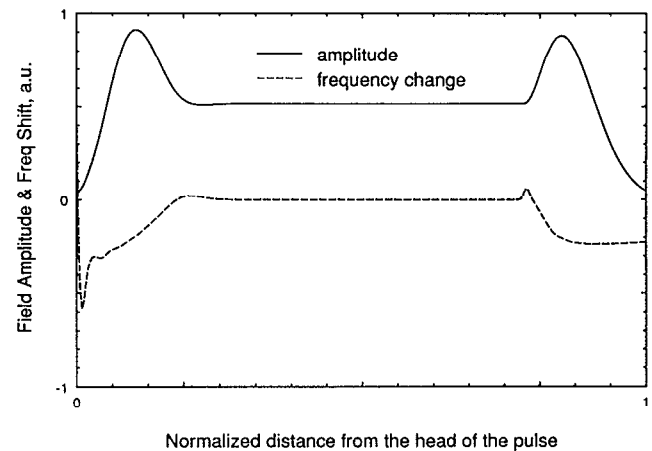


FIG. 6. Spike formation and frequency change, 20 passes after a jump in detuning, as predicted by the simulation code.

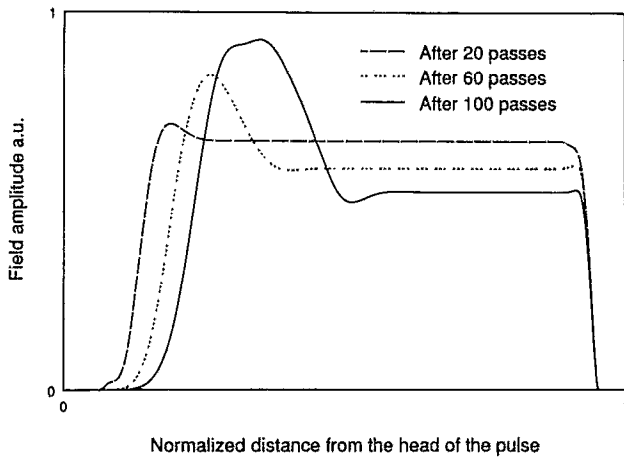


FIG. 7. Pulse evolution for  $5\mu$  cavity detuning.

pulse length and temporal variation of beam parameters requires further research.

There are a number of ways in which the radiation frequency follows the electron energy. The spectrum can adjust itself through amplification of noise and spontaneous emission at the resonant frequency. Or, adjustment can be achieved through the generation of sidebands in a strongly nonlinear regime. Since the numerical studies described in this article were carried out without beam noise and in a regime where the synchrotron length significantly exceeded the wiggler length (ruling out a sideband explanation), the upshifting model appears to be the only satisfactory description of frequency adjustment.

Slippage, which gives the FEL interaction a wake-like nature, generates frequency shifts by producing a time-dependent dielectric coefficient at the edges of the pulse. Physically, this mechanism is the analog of superradiance<sup>4</sup> for a low-gain oscillator. Superradiance in a high-gain FEL is usually associated with a spike which emerges within one slippage length of the trailing edge of the pulse. High gain creates an asymmetry in the evolution of the leading and trailing edges. In a low-gain oscillator, spikes created at the

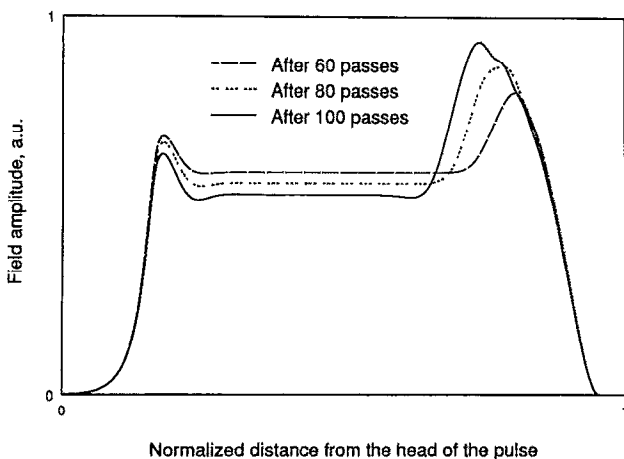


FIG. 8. Pulse evolution for  $25\mu$  cavity detuning.

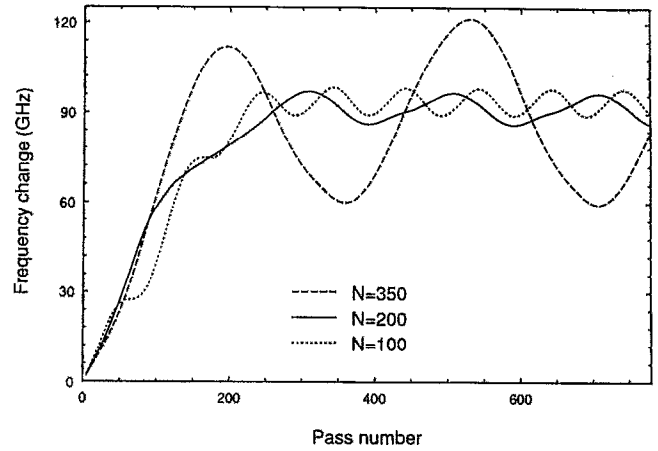


FIG. 9. Output frequency as a function of pass number for an energy variation amplitude of  $\delta\gamma/\gamma=8\times 10^{-2}\%$  and various modulation periods.

edges can propagate into the body of the pulse only one slippage length in one pass (the slippage per pass is small for all the runs). The propagation of the correct frequency into the body of the pulse is through the diffusion mechanism described above. Also, retaining only two  $s$  derivatives in the evolution equation and assuming low gain forces the leading and trailing edges to evolve similarly.

The response of the FEL to energy modulation (or any other slow parameter change) can also be achieved through frequency shifting. Numerical simulations show that, when the electron beam energy  $\gamma$  is varied sinusoidally with the pass number, the number of passes required to respond to a step variation in beam energy,  $N_{\text{resp}}$ , is an important quantity. Then, depending on whether the period of energy modulation is smaller or larger than  $N_{\text{resp}}$ , the amplitude of the output frequency variation will be small or large, respectively. Simulations were performed with a cavity detuning which corresponded to  $N_{\text{resp}} \approx 200$ . We note that, for our parameters,  $N_{\text{resp}}$  is much larger than the cavity  $Q$ . The energy was modulated according to

$$\gamma(N) = \gamma_0 + \delta\gamma \sin(2\pi n/N), \quad (35)$$

where  $N$  is the periodicity of modulation, and  $n$  is the pass number. The results for different values of  $N$  are presented in Fig. 9.

## V. CONCLUSIONS

The amplifier theory presented here explains recent experimental observations<sup>15</sup> of frequency upshifting in a microwave FEL. The theory predicts both the large shifts observed when the FEL is operated in group I orbits, and the small shifts observed in reversed field operation. These phenomena will need to be incorporated into designs of FEL power sources for accelerators, where the phase of the radio-frequency radiation is tightly constrained. This is especially true for the high-energy linear collider designs with multiple bunchlets. Further work on the phase stability will be required if a short-pulse FEL is to be used as an accelerator power source.



Frequency shifting can arise from time dependence in the beam current and energy, as well as from the time dependence introduced in the dielectric coefficient through slippage and finite length of the electron or radiation pulses. Frequency adjustment of an FEL oscillator to a jump in beam energy was studied analytically, with a diffusion equation, and numerically. The predictions of the diffusion model for the rate at which the new FEL frequency establishes itself in the pulse is consistent with the simulation. For present designs, the nonresonant plasma contribution to the dielectric does not seriously limit the FEL bandwidth. With the use of electromagnetic wigglers and microwigglers, the plasma dielectric will become more significant.

## ACKNOWLEDGMENTS

We are grateful to G. Zhang for providing us with her microwave FEL simulation code and to S. Benson for his FEL oscillator code. We have benefited from discussions of experimental results with G. Bekefi, M. Conde, and P. Volfbeyn.

This work was supported by the U.S. Department of Energy, Division of High Energy Physics, and by Lawrence Livermore National Laboratory.

## APPENDIX: DERIVATION OF THE MASTER EQUATION

In this appendix a diffusion-like master equation for the pulse evolution in an FEL oscillator is derived under the assumption of small gain per pass and a power expansion in the slippage parameter. This is equivalent to the assumption that the complex amplitude  $\hat{a}$  does not change significantly over a slippage length. Furthermore, we neglect beam loading, since it is independent of the FEL interaction and can be added *a posteriori*.

We use  $\bar{z}=z/L_w$  as an independent variable, so that the beam enters at  $\bar{z}=0$  and exits at  $\bar{z}=1$ . The dimensionless coordinates, introduced in Eq. (26), assure that

$$\frac{d\bar{s}}{d\bar{z}}=1 \quad (\text{A1})$$

along the unperturbed trajectory. Assuming a plane wave, the ponderomotive phase is

$$\theta=k_{wz}-kc(t-z/c)=2\pi N(\bar{z}-\bar{s})+y_0\bar{s}. \quad (\text{A2})$$

In this notation, the Compton FEL equations<sup>3</sup> are

$$\frac{\partial \hat{a}}{\partial \bar{z}}=\frac{2\pi i a_w L_w r_e \delta n}{\gamma k_z}, \quad (\text{A3})$$

$$\frac{d\theta_j}{d\bar{z}}=y_j,$$

$$\frac{dy_j}{d\bar{z}}=i\frac{16\pi^2 N^2 a_w}{1+a_w^2} \hat{a}[\bar{s}_j(\bar{z}), \bar{z}] \exp(i\theta_j). \quad (\text{A4})$$

In the continuous limit, with  $\theta_0$  the initial particle phase, we can integrate the above equations, in the linear approximation, to obtain

$$\begin{aligned} \theta &= \theta_0 + y_0 \bar{z} + i \frac{4\pi^2 N^2}{1+a_w^2} \int_0^{\bar{z}} d\bar{z}' \int_0^{\bar{z}'} d\bar{z}'' \\ &\quad \times \hat{a}(\bar{s}_0 + \bar{z}'', \bar{z}'') \exp i(y_0 \bar{z}'' + \theta_0). \end{aligned} \quad (\text{A5})$$

Since electrons enter the wiggler unbunched, the density perturbation is

$$\delta n = -n_0 \left( \frac{\partial \theta(\theta_0, \bar{z})}{\partial \theta_0} - 1 \right). \quad (\text{A6})$$

Combining Eqs. (A3), (A5), and (A6) results in

$$\begin{aligned} \frac{\partial \hat{a}}{\partial \bar{z}} &= i j_c \exp(-iy_0 \bar{z}) \int_0^{\bar{z}} d\bar{z}' \int_0^{\bar{z}'} d\bar{z}'' \hat{a}(\bar{s}_0 + \bar{z}'', \bar{z}'') \\ &\quad \times \exp(iy_0 \bar{z}''). \end{aligned} \quad (\text{A7})$$

If the total single-pass gain is less than unity, the variation of  $\hat{a}$  with  $\bar{z}$  in its second argument can be neglected, and, if the field is smooth over a slippage distance, we need only retain up to second derivatives in the first argument of  $\hat{a}$ . With

$$p(s_0, \bar{z}) = \int_0^{\bar{z}} d\bar{z}' \int_0^{\bar{z}'} d\bar{z}'' \exp(iy_0 \bar{z}'') \quad (\text{A8})$$

it can be easily shown that the RHS of Eq. (A7) is

$$\exp(-iy_0 z) \left( \hat{a}(s_0) p - i \frac{\partial \hat{a}(s_0)}{\partial \bar{s}} \frac{\partial p}{\partial y_0} - \frac{1}{2} \frac{\partial^2 \hat{a}(s_0)}{\partial \bar{s}^2} \frac{\partial^2 p}{\partial y_0^2} \right). \quad (\text{A9})$$

Next, we express Eq. (A9) in terms of  $(\bar{s}, \bar{z})$  using Eq. (A1),  $\bar{s}_0 = \bar{s} - \bar{z}$ , and expand the fields in Eq. (A9), keeping only the first two derivatives. Integration over  $\bar{z}$  from zero to unity yields the field increment per pass. Treating the pass number  $n$  as a continuous variable, and taking into account intracavity losses, we obtain the master equation

$$\frac{\partial \hat{a}}{\partial n} = -\delta \hat{a} + \hat{a} \hat{G} - i \frac{\partial \hat{a}}{\partial \bar{s}} \frac{d\hat{G}}{dy_0} - \frac{1}{2} \frac{\partial^2 \hat{a}}{\partial \bar{s}^2} \frac{d^2 \hat{G}}{dy_0^2}. \quad (\text{A10})$$

Equation (A10) is not causal. Thus, if we start with a pulse extending from  $s=0$  back into the region of positive  $s$ , Eq. (A10) predicts that the pulse will spread into a region of negative  $s$  as well, which clearly is not physical. To remain causal, all the higher derivatives,  $(\partial^n \hat{a} / \partial \bar{s}^n)$ , of the field must be kept.

In principle, all the higher-order derivatives can be taken into account and an extended master equation can be solved by Fourier transform. Neglecting the change of  $\hat{a}$  with  $z''$  in Eq. (A7), we can integrate it to obtain the coarse-grained equation for  $\hat{a}(s, n)$

$$\begin{aligned} \frac{\partial \hat{a}}{\partial n} &= i j_c \int_0^1 d\bar{z} \int_0^{\bar{z}} d\bar{z}' \int_0^{\bar{z}'} d\bar{z}'' \hat{a}(\bar{s} + \bar{z}'' - \bar{z}) \\ &\quad \times \exp[iy_0(\bar{z}'' - \bar{z})]. \end{aligned} \quad (\text{A11})$$

We then expand  $\hat{a}(s + z'' - z)$  around  $s$  to all powers of  $(z'' - z)$  and Fourier transform the resulting infinite series in  $s$ . Introducing

$$\hat{a}(\omega, n) = \int_{-\infty}^{+\infty} ds \exp(i\omega s) \hat{a}(s, n), \quad (\text{A12})$$

we obtain

$$\frac{\partial \hat{a}(\omega, n)}{\partial n} = ij_c \hat{a}(\omega, n) \sum_{n=0}^{\infty} \frac{(-i\omega)^n}{n!} \int_0^1 d\bar{z} \int_0^{\bar{z}} d\bar{z}' \int_0^{\bar{z}'} d\bar{z}'' \times (z'' - z)^n \exp[iy_0(\bar{z}'' - \bar{z})]. \quad (\text{A13})$$

It is straightforward to see that, using the definition of the complex gain function  $\hat{G}$  from Eq. (28), Eq. (A13) can be rewritten as

$$\frac{\partial \hat{a}(\omega, n)}{\partial n} = \hat{a}(\omega, n) \sum_{n=0}^{\infty} \frac{(-\omega)^n}{n!} \frac{d^n \hat{G}(y_0)}{dy_0^n}. \quad (\text{A14})$$

The infinite series in the RHS of Eq. (A14) is the Taylor expansion of the function  $\hat{G}(y_0 - \omega)$ . Integrating in  $n$  and Fourier transforming back into  $s$  space we obtain the solution to the extended master equation

$$\hat{a}(n, s) = \int_{-\infty}^{+\infty} ds' \mathcal{G}_n(s - s') \hat{a}(0, s'), \quad (\text{A15})$$

where  $\mathcal{G}_n$  is a Green's function of the FEL interaction, having the causal property of  $\mathcal{G}_n(s) = 0$  for  $s < 0$ . The Green's function is given by the following expression:

$$\mathcal{G}_n = \frac{1}{2\pi} \int_C d\omega \exp[-i\omega s + g(\omega)n], \quad (\text{A16})$$

where the integral is taken along a contour in the upper half of the complex plane and

$$g(\omega) = \hat{G}(y_0 - \omega), \quad (\text{A17})$$

with  $\hat{G}$  defined in Eq. (28). It is straightforward to show that  $g(\omega)$  is well behaved in the upper half plane, so that the Green's function is causal. Analyzing a low- $Q$  cavity with our model should not lead to any spurious results since radiation that moves ahead of the beam will decay in a few passes.

As is easy to see from Eq. (A10), the nonlocal character of the FEL interaction introduces dispersion (a second-derivative term) into Eq. (A10). We note that the growth of the diffusion coefficient as the fourth power of

the total number of wiggler periods reflects our assumption of total gain less than unity. When this condition is violated, the diffusion coefficient becomes independent of the number of wiggler periods, since, for the high-gain FEL, the "communication distance" between different radiation slices is no longer  $N_w \lambda_w / 2\gamma_{\parallel}^2$ , but rather the coherence length (Ref. 4),  $\approx 1/\Gamma 2\gamma_{\parallel}^2$ .

- <sup>1</sup>K.-J. Kim and M. Xie, Nucl. Instrum. Methods A **304**, 146 (1991).
- <sup>2</sup>R. W. Kuenning, A. M. Sessler, and J. S. Wurtele, *Laser Acceleration of Particles*, Malibu, CA, edited by C. Joshi and T. Katsouleas (American Institute of Physics, New York, 1985), p. 324.
- <sup>3</sup>W. B. Colson, IEEE J. Quantum Electron. **QE-17**, 1417 (1981).
- <sup>4</sup>R. Bonifacio and F. Casagrande, Nucl. Instrum. Methods A **239**, 36 (1985); R. Bonifacio, N. Piovella, and B. W. J. McNeil, Phys. Rev. A **44**, 3441 (1991).
- <sup>5</sup>S. C. Wilks, J. M. Dawson, and W. B. Mori, Phys. Rev. Lett. **61**, 337 (1989).
- <sup>6</sup>Wm. M. Wood, C. W. Siders, and M. C. Downer, Phys. Rev. Lett. **67**, 3523 (1991).
- <sup>7</sup>R. L. Savage, Jr., C. Joshi, and W. B. Mori, Phys. Rev. Lett. **68**, 946 (1992).
- <sup>8</sup>M. E. Conde, C. J. Taylor, and G. Bekefi, Phys. Fluids B **2**, 1934 (1993).
- <sup>9</sup>C. B. Darrow, C. Coverdale, M. D. Perry, W. B. Mori, C. Clayton, K. Marsh, and C. Joshi, Phys. Rev. Lett. **69**, 442 (1992).
- <sup>10</sup>C. W. Roberson and P. Sprangle, Phys. Fluids B **1**, 3 (1989).
- <sup>11</sup>E. Esarey, A. Ting, and P. Sprangle, Phys. Rev. A **42**, 3526 (1990).
- <sup>12</sup>M. Lampe, E. Ott, and J. H. Walker, Phys. Fluids **21** 42 (1978).
- <sup>13</sup>J. S. Wurtele, R. Chu, and J. Fajans, Phys. Fluids B **2**, 1626 (1990).
- <sup>14</sup>E. Esarey, G. Joyce, and P. Sprangle, Phys. Rev. A **44**, 3908 (1991).
- <sup>15</sup>M. W. Conde and G. Bekefi, IEEE Trans. Plasma Sci. **PS-20**, 240 (1992).
- <sup>16</sup>P. Volfbeyn, K. Ricci, B. Chen, and G. Bekefi, IEEE Trans. Plasma Sci. (in press).
- <sup>17</sup>G. Zhang, G. Shvets, and J. S. Wurtele, Nucl. Instrum. Methods A **331**, 472 (1993).
- <sup>18</sup>H. Al-Abawi, J. K. McIver, G. T. Moore, and M. O. Scully, in *Physics of Quantum Electronics*, edited by S. F. Jacobs, H. S. Pilloff, M. O. Scully, G. T. Moore, M. Sargent, III, and R. Spitzer (Addison-Wesley, Reading, MA, 1980), Vol. 9, p. 415.
- <sup>19</sup>S. V. Benson, Ph.D. dissertation, Department of Physics, Stanford University, 1985.
- <sup>20</sup>G. Dattoli, J. C. Gallardo, A. Renieri, and A. Torre, Phys. Rev. A **35**, 4175 (1987); G. Dattoli, J. C. Gallardo, T. Hermsen, A. Renieri, and A. Torre, *ibid.* **37**, 4326 (1988); G. Dattoli, T. Hermsen, L. Mezi, A. Renieri, and A. Torre, *ibid.* **37**, 4334 (1988).